

839

V393  
.R46

MIT LIBRARIES



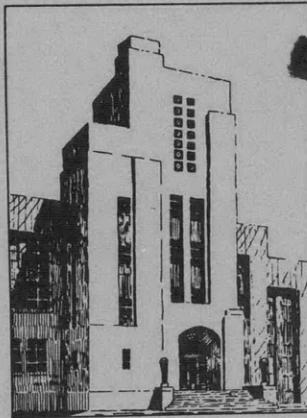
852

NAVY DEPARTMENT  
THE DAVID W. TAYLOR MODEL BASIN  
WASHINGTON 7, D.C.

LARGE ELASTIC BENDING  
OF HEAVY, UNIFORM CANTILEVERS  
WITH HYDRODYNAMIC LOADING

by

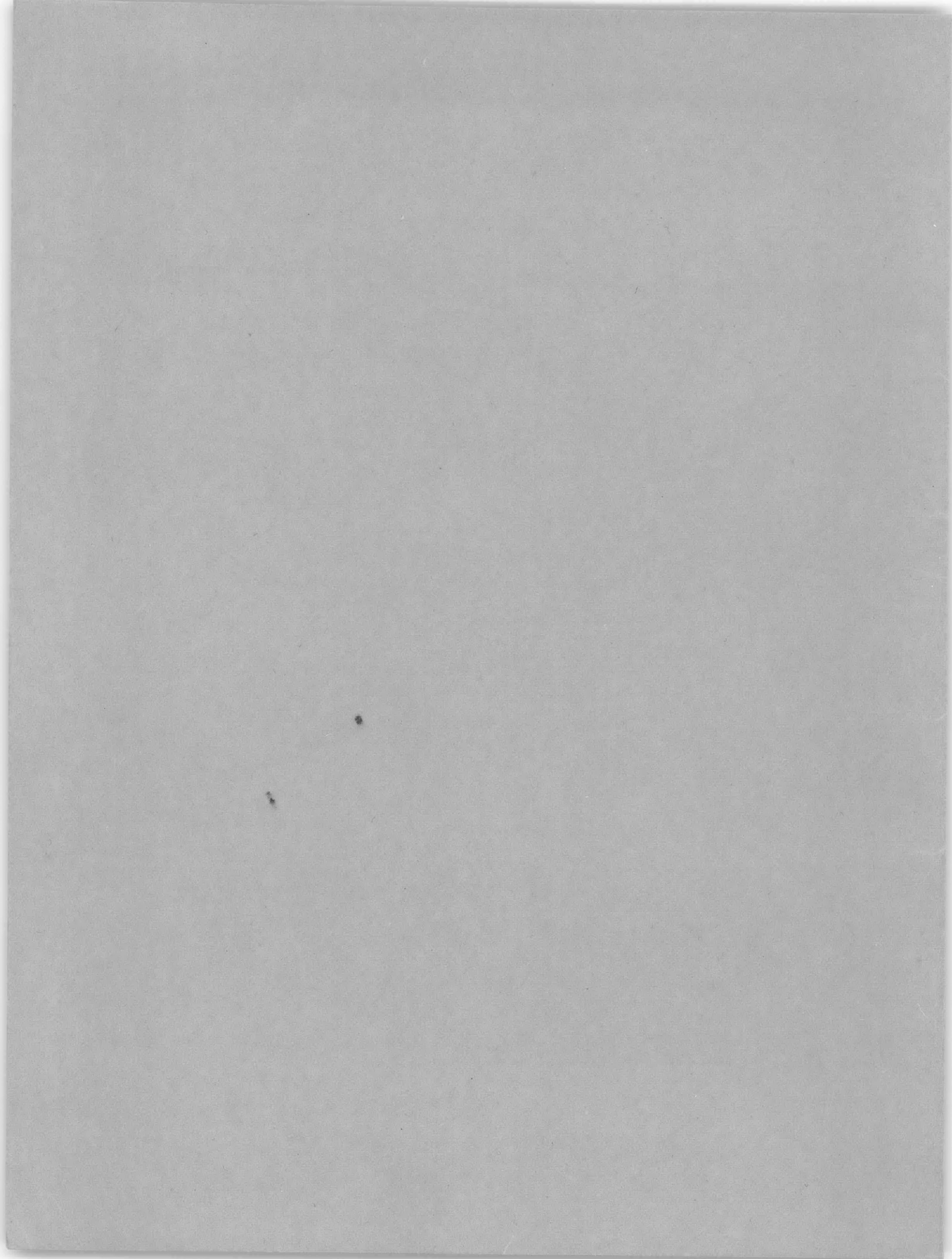
Phillip Eisenberg and L. Folger Whicker



November 1952

Report 839

NE 091-010



## NOTATION

|             |  |
|-------------|--|
| $c$         | $\sqrt[3]{\frac{EI}{R}}$ , a characteristic length                                 |
| $C_D$       | Drag coefficient   |
| $d$         | A characteristic section length, e.g., diameter of a cylinder                      |
| $E$         | Modulus of elasticity in tension and compression, assumed to be same as in bending |
| $h$         | Depth of beam in plane of bending  |
| $I$         | Section moment of inertia  |
| $M$         | Bending moment   |
| $R_d$       | $Ud/\nu$ , Reynolds number   |
| $R$         | Drag per unit length of beam when normal to direction of motion                    |
| $S$         | Shear force  |
| $S_{bend}$  | Bending stress   |
| $s$         | Distance along cantilever measured from free end                                   |
| $T$         | Tensile force  |
| $U$         | Velocity of cantilever   |
| $W$         | Weight per unit length of beam   |
| $x, y$      | Cartesian coordinates of deformed beam   |
| $\zeta$     | $s/c$ , dimensionless length along cantilever                                      |
| $\theta$    | Slope of beam  |
| $\mu$       | $Mc/EI$ , dimensionless bending moment   |
| $\nu$       | Kinematic viscosity of fluid   |
| $\xi, \eta$ | $x/c, y/c$ , dimensionless cartesian coordinates of beam                           |
| $\rho$      | Mass density of fluid or radius of curvature of beam, as indicated                 |
| $\sigma$    | $S/cR$ , dimensionless shear force   |
| $\tau$      | $T/cR$ , dimensionless tensile force   |
| $\phi$      | Angle between tangent to beam and direction of motion                              |

*See* 025163

$\psi$   $\frac{S_{bend}}{E} \cdot \frac{s}{h} = \frac{1}{2} \mu \zeta$ , dimensionless bending stress

$\omega$   $W/R$ , ratio of weight per unit length to drag per unit length

Subscript 0 Refers to values at free end of beam

# LARGE ELASTIC BENDING OF HEAVY, UNIFORM CANTILEVERS WITH HYDRODYNAMIC LOADING\*

by

Phillip Eisenberg and L. Folger Whicker

## ABSTRACT

Much work has been done on the shape of and tension in flexible members (bending neglected) loaded by the forces arising during motion in a fluid. In this report, computations are extended to the case of elastic members, and results are derived for the shape, bending moments, and shear of a uniform cantilever. The beam is assumed to be symmetrical about and to bend only in the plane of motion.

The loading is made up of the weight of the bar and the hydrodynamic force. The latter is assumed to follow the "sine-squared law," i.e., unit loading is  $R \sin^2 \phi$  where  $R$  is the drag per unit length of beam when normal to the direction of motion and  $\phi$  is the angle between the tangent to the bar and the direction of motion. Assuming the applicability of the Bernoulli-Euler law, assuming linear Hooke's law and no change in total length of beam, neglecting warping of the sections, and neglecting the tangential forces, the slope of the beam as a function of the distance along the beam is derived in the form of a nonlinear integro-differential equation. An approximate solution is obtained by expansion in a Maclaurin's series in which the coefficients of the first ten terms are evaluated.

Values of total shear are compared with experimental results for the drag of cantilevers with circular sections obtained from towing tests. The theoretical and experimental results are shown to be in good agreement for those cases in which available drag coefficients apply, i.e., for nonvibrating beams, and for which the slopes at the free ends were as high as 63 degrees.

Tables and curves of values of slope, non-dimensional shear, moment, and bending stress as a function of non-dimensional length are given for cantilevers without end loading for various ratios of weight to hydrodynamic drag. Coefficients of the solution for cantilevers loaded at the end with forces and moments are tabulated in the Appendix.

---

\*An abstracted version of this report giving only the results for cantilevers with ends not loaded was presented before the Virginia Academy of Sciences on 16 May 1952.

## INTRODUCTION

There are a large number of applications relating to the towing of devices at sea or in a stream which require knowledge of the shape and forces in the cable or strut used for towing. Much work has been done on the shape and tension of flexible cables (bending neglected) loaded by the forces arising during motion in a fluid,<sup>1,2</sup> and these can now be computed with considerable accuracy. However, no results are available for the shape of and stresses in elastic members used in such applications when the deflections are so large that linearized beam theory is no longer valid.

In this paper, the intention is to test the accuracy of a solution using the usual linearizing assumptions of elastic beam theory but making no initial approximations in the curvature term of the Bernoulli-Euler equation. Furthermore, it is assumed that the strut is not subject to vibration arising from interaction with its wake, so that the solution is valid only for those cases in which the natural frequencies of the strut are not near the wake frequencies. The computations are further restricted to cantilevers assumed to be symmetrical about and to bend only in the plane of motion.

## DERIVATION OF THE ELASTIC EQUATION

The hydrodynamic loading is assumed to follow the "sine-squared law," i.e., the unit loading is  $R \sin^2 \phi$  where  $R$  is the drag per unit length of beam when normal to the direction of motion and  $\phi$  is the angle between the tangent to the beam and the direction of motion. Except for very small angles (< 10 deg.) of inclination to the stream, this result is well established by experimental evidence and supported by theoretical considerations.<sup>3,4</sup> Here,

$$R = \frac{1}{2} \rho U^2 d C_D$$

where  $\rho$  is the mass density of the fluid,

$U$  is the towing speed,

$d$  is a characteristic section dimension of the strut, and

$C_D = C_D(R_d)$  is the drag coefficient (function of Reynolds number  $R_d = \frac{Ud}{\nu}$ , where  $\nu$  is the kinematic viscosity of the fluid).

The tangential component of the hydrodynamic force has been found to be small in comparison with the normal force when the angle of inclination over most of the strut is reasonably large (> 10 - 15 deg.), and will be neglected. An assumption that has not been directly verified is

---

<sup>1</sup>References are listed on page 22.

implicit in the present work. The sine-squared law has been verified for bars and stranded cables with no curvature; it is assumed here that this law applies locally everywhere on the deformed beam. However, the fact that this has given accurate results in flexible-cable problems is sufficient evidence, though indirect, of its validity.

The coordinate system used and the forces acting on an element of the strut of length  $ds$  are illustrated in Figures 1 and 2. The origin of coordinates is taken at the free end of the cantilever,  $s = 0$ ,  $\theta = \theta_0$ .  $T$ ,  $S$ , and  $M$  denote the axial force, shear force, and moment, respectively, and  $W$  is the weight per unit length. Equilibrium requires, for the horizontal forces,

$$d(T \cos \theta) - d(S \sin \theta) = - (R \cos^2 \theta \sin \theta + W) ds$$

which, upon integration and evaluation of the integration constant at the origin, yields,

$$T \cos \theta - S \sin \theta = -R \int_0^s \cos^2 \theta \sin \theta ds - Ws + T_0 \cos \theta_0 - S_0 \sin \theta_0 \quad [1]$$

For the vertical forces,

$$d(T \sin \theta) + d(S \cos \theta) = R \cos^3 \theta ds$$

and, integrating,

$$T \sin \theta + S \cos \theta = R \int_0^s \cos^3 \theta ds + T_0 \sin \theta_0 + S_0 \cos \theta_0 \quad [2]$$

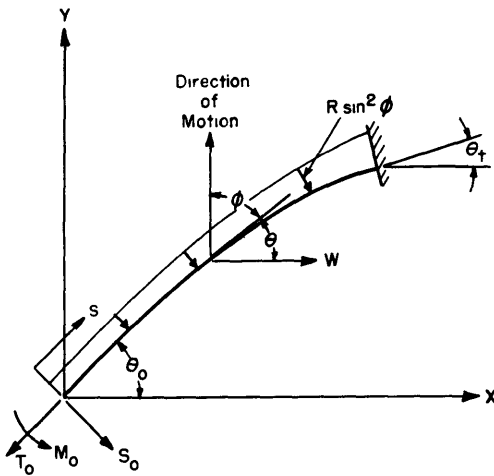


Figure 1 - Coordinate System and Assumed Loading

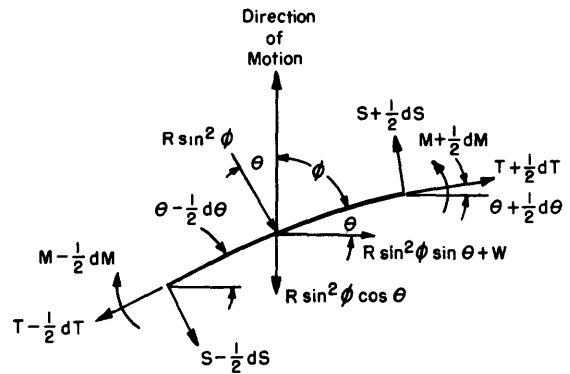


Figure 2 - Force Diagram

In summing moments it is assumed that the contribution due to change in axial force along the beam may be neglected in comparison with those of the weight and normal forces. This is, of course, equivalent to the usual assumption of small curvature of linearized beam theory. However, this has been used in similar problems with excellent results.<sup>5\*</sup> Thus

$$-S = \frac{dM}{ds} \quad [3]$$

Finally, to obtain the equation of the elastic curve, we take the Bernoulli-Euler result,\*\*

$$\frac{d\theta}{ds} = \frac{M}{EI} \quad [4]$$

(since we are considering only beams that are long compared with any section dimension). Here,  $E$  is the modulus of elasticity in tension and compression and  $I$  is the section moment of inertia.

Eliminating  $T$  between [1] and [2] and combining the result with [3] and [4] to eliminate  $S$  gives

$$\begin{aligned} -\frac{S}{R} = \frac{EI}{R} \frac{d^2\theta}{ds^2} = \sin\theta \left\{ -\int_0^s \cos^2\theta \sin\theta ds - \frac{Ws}{R} + \frac{T_0}{R} \cos\theta_0 - \frac{S_0}{R} \sin\theta_0 \right\} \\ - \cos\theta \left\{ \int_0^s \cos^3\theta ds + \frac{T_0}{R} \sin\theta_0 + \frac{S_0}{R} \cos\theta_0 \right\} \end{aligned}$$

Put

$$\frac{EI}{R} = c^3, \quad \frac{T_0}{cR} = \tau_0, \quad \frac{S_0}{cR} = \sigma_0, \quad \frac{W}{R} = \omega, \quad \xi = \frac{x}{c}, \quad \eta = \frac{y}{c}, \quad \zeta = \frac{s}{c} \quad [5]$$

---

\*Bickley's<sup>5</sup> results have also been verified experimentally by Mr. J.S. Brock of the David Taylor Model Basin.

\*\*It has been shown by Seth<sup>6</sup> that for large curvature the bending moment formula must be modified to include second order terms of the type,  $\text{const. } h^2/\rho^3$ , where  $h$  is the depth of the beam and  $\rho$  is the radius of curvature. An examination of the final results indicates that neglecting these terms is justified within the approximations of the present solution and within the elastic range of ordinary steels, i.e., before failure occurs, as indicated from observations during the experiments cited.



The shape of the strut is then given by\*

$$\begin{aligned} \frac{d^2\theta}{d\xi^2} = \sin\theta \left\{ -\int_0^\xi \cos^2\theta \sin\theta d\xi - \omega\xi + \tau_0 \cos\theta_0 - \sigma_0 \sin\theta_0 \right\} \\ - \cos\theta \left\{ \int_0^\xi \cos^3\theta d\xi + \tau_0 \sin\theta_0 + \sigma_0 \cos\theta_0 \right\} \end{aligned} \quad [6]$$

or, to the present degree of approximation, by

$$\xi = \int_0^\xi \cos\theta d\xi$$

and

$$\eta = \int_0^\xi \sin\theta d\xi \quad [7]$$

### APPROXIMATE SOLUTION OF THE ELASTIC EQUATION

An approximate solution of Equation [6] will be found by expansion in a Maclaurin's series:\*\*

$$\theta(\xi) = \theta(0) + \xi\theta'(0) + \frac{\xi^2}{2!}\theta''(0) + \dots \quad [8]$$

with the boundary conditions at  $s = 0$ :  $\theta = \theta_0$  and  $M = M_0$ .

The first ten coefficients are tabulated in the Appendix.

For purposes of testing the approximate solution, it is convenient to consider only cantilevers without end loading, i.e.,  $T_0 = S_0 = M_0 = 0$ . This assumes that there is no additional loading at the free end when towed as a free cantilever. However, the flow around the free end actually introduces a force  $T_0$  which will be largest when the free end is nearly normal to

---

\*The equation as derived is treated directly in the following section. For the approximate methods used, there is no advantage in reducing it to its differential form:

$$\begin{aligned} \frac{d\theta}{d\xi} \frac{d^4\theta}{d\xi^4} + \left(\frac{d\theta}{d\xi}\right)^3 \frac{d^2\theta}{d\xi^2} - \frac{d^2\theta}{d\xi^2} \frac{d^3\theta}{d\xi^3} = \cos\theta \left(\frac{d\theta}{d\xi}\right)^2 \left\{ 2 \sin^3\theta - 3 \cos^2\theta - \cos^3\theta \cot\theta \right. \\ \left. + 4 \sin\theta \cos\theta - 2\omega \right\} - \cos^2\theta \sin^2\theta \left(\frac{d\theta}{d\xi}\right)^2 \frac{d^2\theta}{d\xi^2} + (\omega \sin\theta + \cos^4\theta) \frac{d^2\theta}{d\xi^2} + \cos^2\theta \cot\theta \end{aligned}$$

\*\*This procedure was also suggested by McLachlan<sup>7</sup> for the solution of the heavy elastica. Bickley<sup>5</sup> obtained results for the latter problem by numerical integration.

the stream direction, i.e., at low speeds, and will decrease (relative to  $R$ ) as  $\theta_0$  increases. As a result, this effect will be small compared with that of the normal forces and will be neglected. Thus, in this case, the first ten coefficients are:

$$\theta(0) = \theta_0$$

$$\theta'(0) = 0$$

$$\theta''(0) = 0$$

$$\theta'''(0) = -\omega \sin \theta_0 - \cos^2 \theta_0$$

$$\theta^{IV}(0) = 0$$

$$\theta^V(0) = 0$$

$$\theta^{VI}(0) = 4 \omega^2 \sin \theta_0 \cos \theta_0 + 2 \omega \cos \theta_0 (2 \cos^2 \theta_0 - \sin^2 \theta_0) - 2 \sin \theta_0 \cos^3 \theta_0 \quad [9]$$

$$\theta^{VII}(0) = 0$$

$$\theta^{VIII}(0) = 0$$

$$\begin{aligned} \theta^{IX}(0) = & 2 \omega^3 \sin \theta_0 (35 \sin^2 \theta_0 - 14 \cos^2 \theta_0) \\ & - \omega^2 (28 \cos^4 \theta_0 + 20 \sin^4 \theta_0 - 227 \sin^2 \theta_0 \cos^2 \theta_0) \\ & + 2 \omega \sin \theta_0 \cos^2 \theta_0 (111 \cos^2 \theta_0 - 22 \sin^2 \theta_0) \\ & + 65 \cos^6 \theta_0 - 24 \sin^2 \theta_0 \cos^4 \theta_0 \end{aligned}$$

so that, to this degree of approximation

$$\theta = \theta_0 + \frac{\xi^3}{3!} \theta'''(0) + \frac{\xi^6}{6!} \theta^{VI}(0) + \frac{\xi^9}{9!} \theta^{IX}(0) \quad [10]$$

The effect of the last term in Equation [10] is very small up to  $\zeta \approx 3$  and  $\theta_f = 0$  deg. for all  $\omega$ . At  $\zeta \approx 5$ , the last term approaches the same order as the other terms, but this is already beyond the range of ordinary applications. However, it is not immediately evident that the terms of higher order are negligible nor that the series so obtained is convergent. The form of the general term is not known, and convergence cannot be tested analytically for Equation [6]. As a result, experiments were conducted to determine the accuracy of the above results. These experiments are described in a subsequent section.

Values of  $\theta$  as a function of  $\theta_0$  with  $\zeta$  as parameter for values of  $\omega$  from  $-1.0$  to  $+1.0$  are given in Table 1 and plotted in Figures 3 through 13. Curves of  $\theta_0$  as a function of  $\zeta$  with  $\omega$  as parameter for the case of a strut with the fixed end normal to the direction of motion (i.e.,  $\theta = 0$  deg. at the fixed end) are shown in Figure 14. The points on Figures 3 through 8 at which  $\theta = \theta_0$  (independent of  $\zeta$ ), i.e., for negative  $\omega$ , represent the conditions under which the hydrodynamic forces just balance the weight of the strut. This point can be obtained from

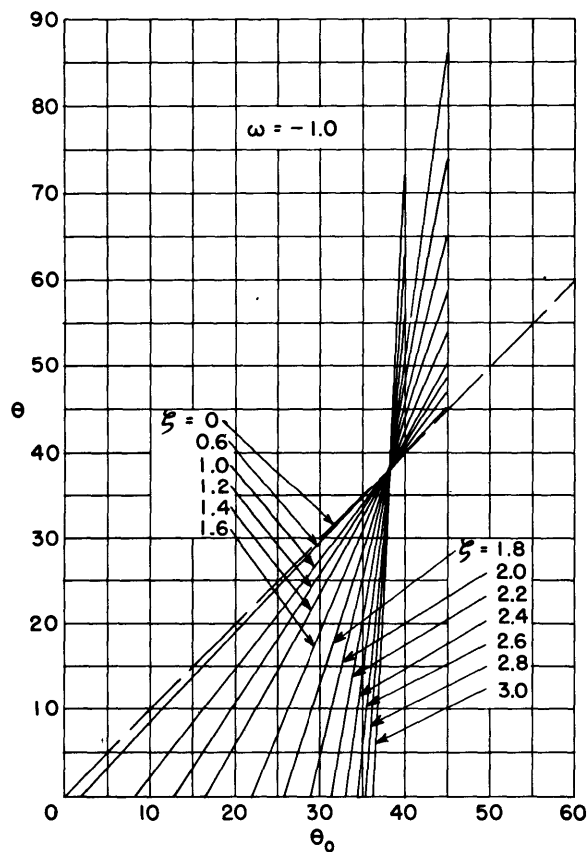


Figure 3 -  $\theta$  versus  $\theta_0$  for  $\omega = -1.0$   
(No End Loading)

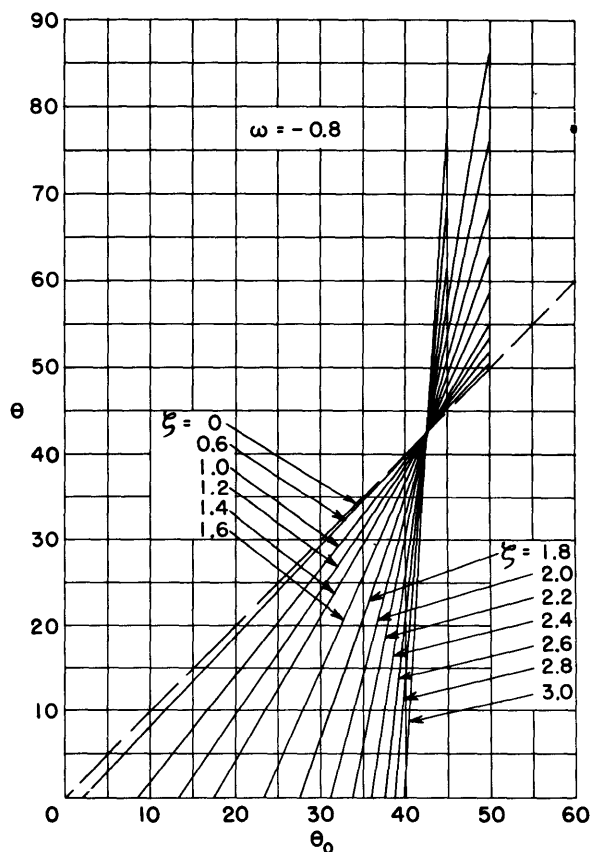


Figure 4 -  $\theta$  Versus  $\theta_0$  for  $\omega = -0.8$   
(No End Loading)





TABLE 1 (Continued)

| $\omega$ | $\theta$<br>degrees | 0.6    | 1.0    | 1.2    | 1.4    | 1.6    | 1.8    | 2.0    | 2.2    | 2.4    | 2.6     | 2.8     | 3.0     |
|----------|---------------------|--------|--------|--------|--------|--------|--------|--------|--------|--------|---------|---------|---------|
| -0.8     | 0                   |        |        |        |        |        |        |        |        |        |         |         |         |
|          | 5                   | 3.085  |        |        |        |        |        |        |        |        |         |         |         |
|          | 10                  | 8.275  | 1.837  |        |        |        |        |        |        |        |         |         |         |
|          | 15                  | 13.493 | 7.862  | 2.409  |        |        |        |        |        |        |         |         |         |
|          | 20                  | 18.730 | 14.004 | 9.416  | 2.700  |        |        |        |        |        |         |         |         |
|          | 25                  | 23.997 | 20.243 | 16.600 | 11.260 | 3.685  |        |        |        |        |         |         |         |
|          | 30                  | 29.274 | 26.556 | 23.917 | 20.052 | 14.550 | 6.888  |        |        |        |         |         |         |
|          | 35                  | 34.598 | 32.914 | 31.317 | 28.976 | 25.651 | 21.017 | 14.627 |        |        |         |         |         |
|          | 40                  | 39.849 | 39.287 | 38.742 | 37.944 | 36.814 | 35.24  | 33.076 | 5.859  | -6.142 | -22.564 |         |         |
|          | 45                  | 45.136 | 45.645 | 46.136 | 46.853 | 47.866 | 49.270 | 51.190 | 53.802 | 57.345 | 62.143  | 13.542  | 2.647   |
|          | 50                  | 50.414 | 51.955 | 53.441 | 55.600 | 58.637 | 62.816 | 68.485 | 76.106 | 86.308 | 99.901  | 118.010 | 141.996 |
| -1.0     | 0                   |        |        |        |        |        |        |        |        |        |         |         |         |
|          | 5                   | 3.119  |        |        |        |        |        |        |        |        |         |         |         |
|          | 10                  | 8.345  | 2.127  |        |        |        |        |        |        |        |         |         |         |
|          | 15                  | 13.599 | 8.328  | 3.174  |        |        |        |        |        |        |         |         |         |
|          | 20                  | 18.875 | 14.644 | 10.501 | 4.372  |        |        |        |        |        |         |         |         |
|          | 25                  | 24.171 | 21.052 | 17.996 | 13.472 | 6.964  | -2.237 |        |        |        |         |         |         |
|          | 30                  | 29.480 | 27.530 | 25.612 | 22.777 | 18.698 | 12.921 | 4.805  | -6.562 |        |         |         |         |
|          | 35                  | 34.800 | 34.037 | 33.293 | 32.191 | 30.611 | 28.355 | 25.242 | 20.624 | 14.735 | 6.174   | -5.819  | -22.562 |
|          | 40                  | 40.124 | 40.552 | 40.930 | 41.610 | 42.510 | 43.774 | 45.542 | 48.000 | 51.420 | 56.167  | 62.776  | 71.940  |
|          | 45                  | 45.457 | 47.041 | 48.610 | 50.914 | 54.197 | 58.791 | 65.147 | 73.890 | 85.880 | 102.305 | 124.780 | 155.477 |

Equation [10] or directly from the diagram of Figure 2. This condition requires that

$$R \sin^2 \phi = W \cos \left( \frac{\pi}{2} - \theta \right)$$

or

$$\omega = - \cos \theta \cot \theta \quad [11]$$

Equation [9] is plotted in Figure 15 and represents the conditions for zero bending stress.

### SHEAR FORCE, BENDING MOMENT, AND BENDING STRESS FOR CANTILEVER WITH NO LOADING AT FREE END

The shear force is found from

$$\sigma = \frac{S}{cR} = \sin \theta_z \left\{ \int_0^{\xi} \cos^2 \theta (\mu) \sin \theta (\mu) d\mu + \omega \xi \right\} \quad [12]$$

$$+ \cos \theta_z \int_0^{\xi} \cos^3 \theta (\mu) d\mu$$

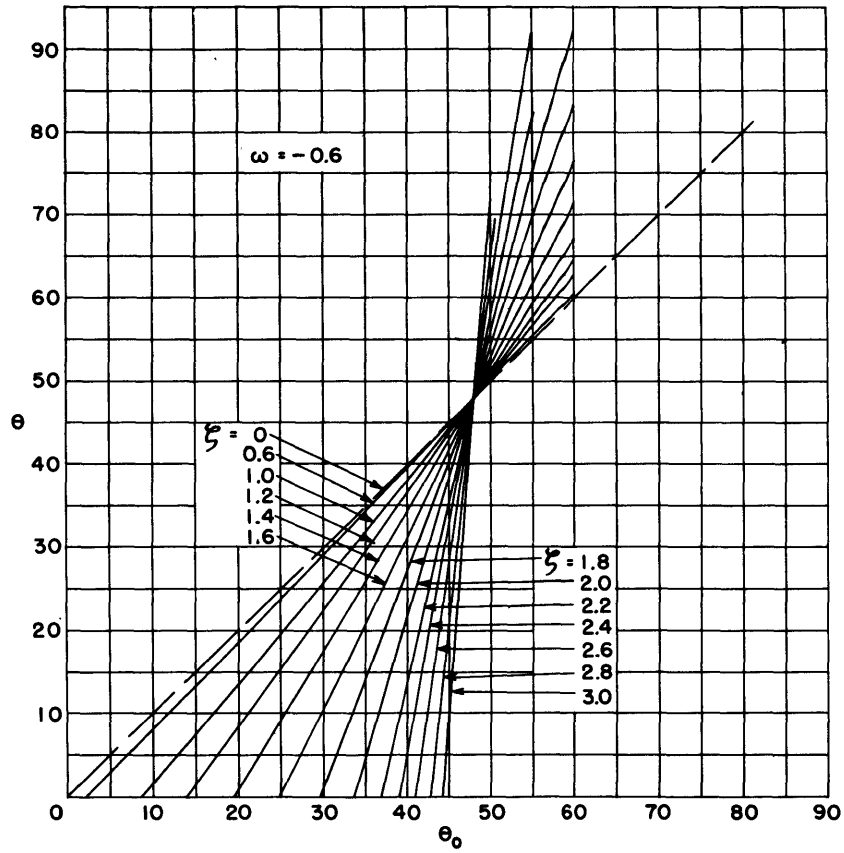


Figure 5 -  $\theta$  Versus  $\theta_0$  for  $\omega = -0.6$  (No End Loading)

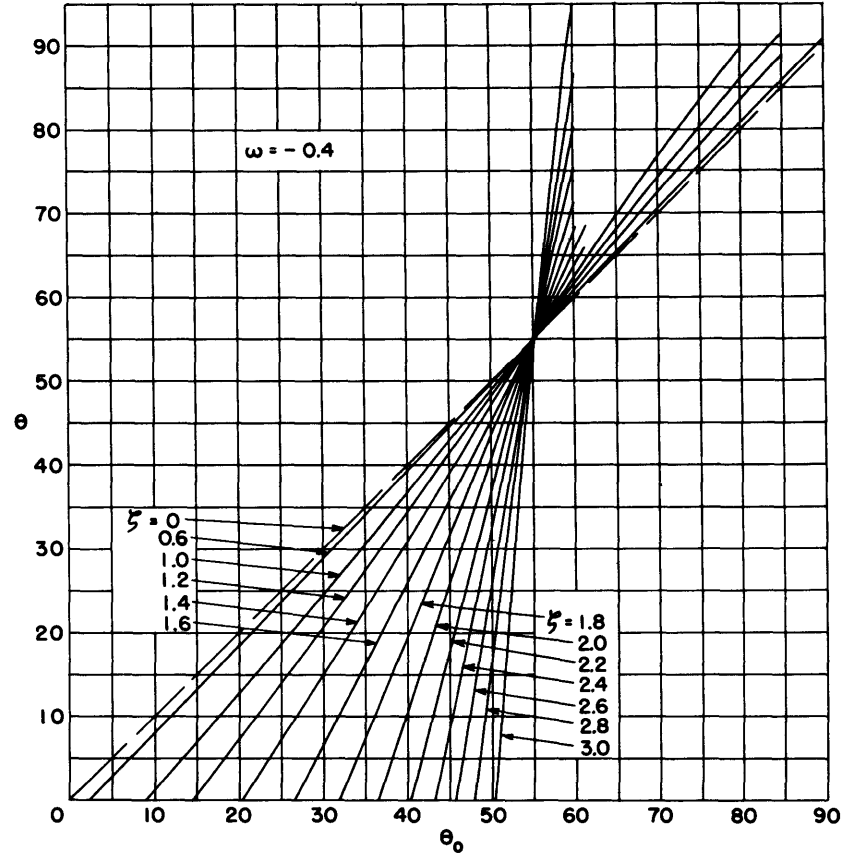


Figure 6 -  $\theta$  Versus  $\theta_0$  for  $\omega = -0.4$  (No End Loading)

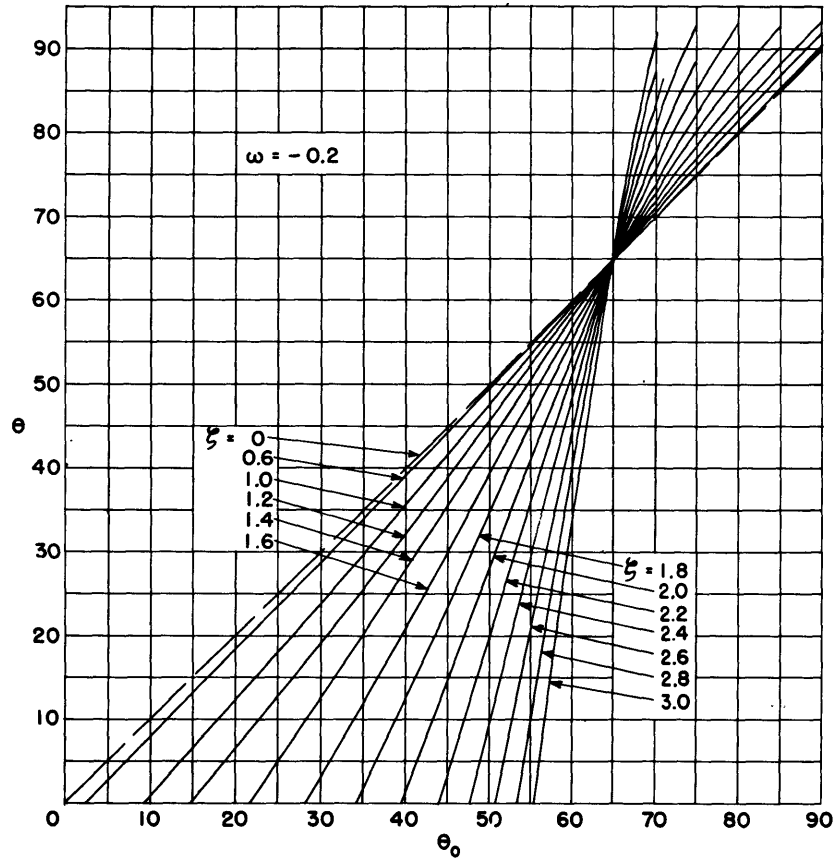


Figure 7 -  $\theta$  Versus  $\theta_0$  for  $\omega = -0.2$  (No End Loading)

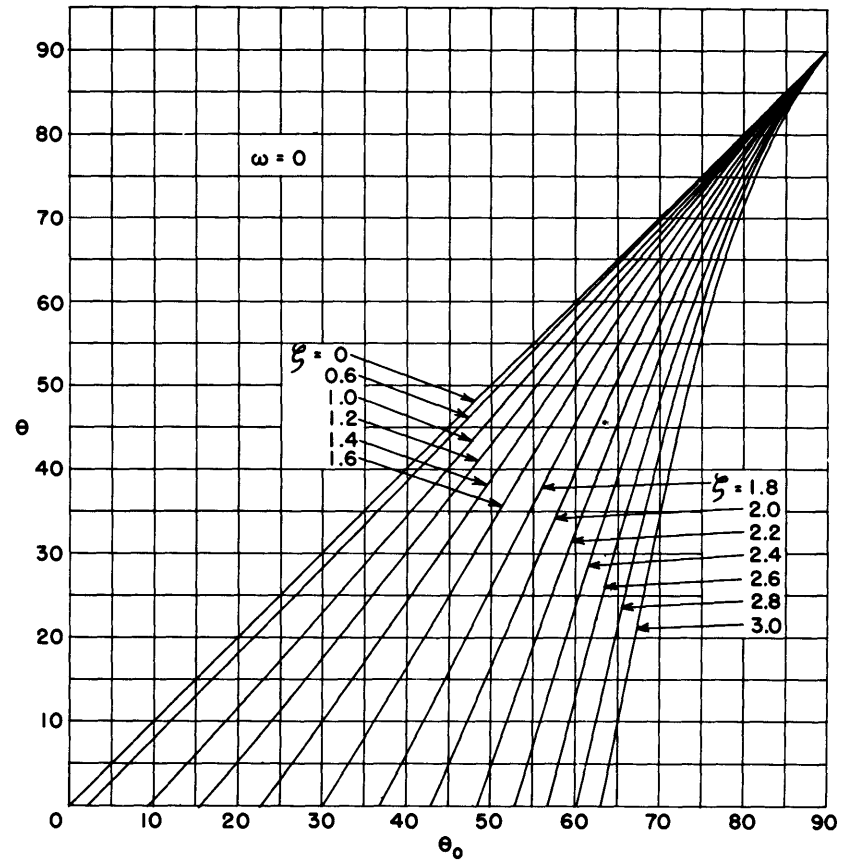


Figure 8 -  $\theta$  Versus  $\theta_0$  for  $\omega = 0$  (No End Loading)



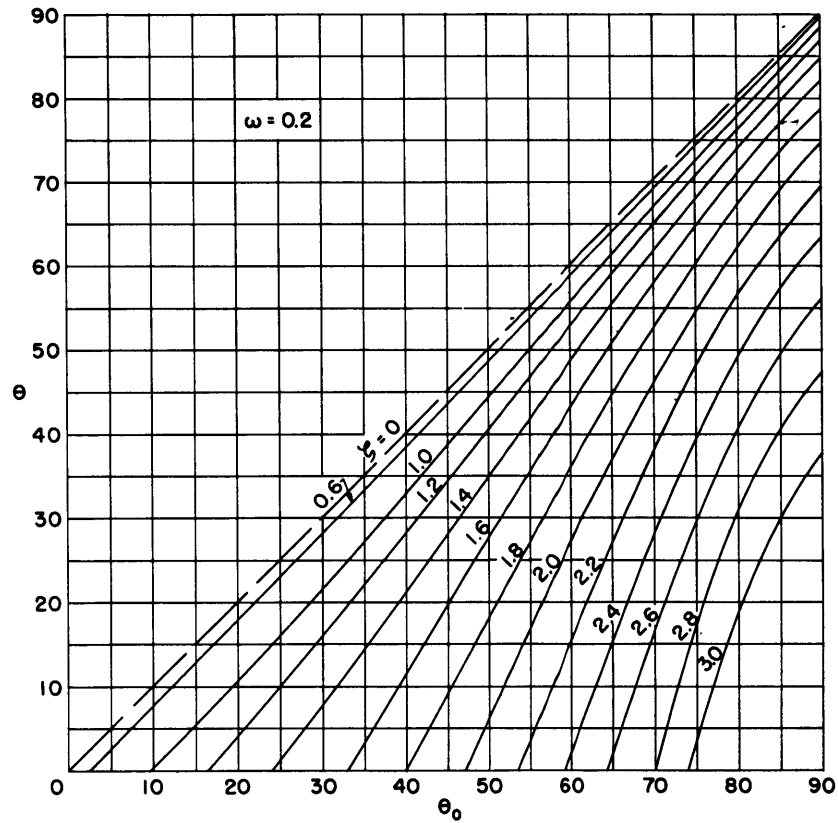


Figure 9 -  $\theta$  Versus  $\theta_0$  for  $\omega = 0.2$  (No End Loading)

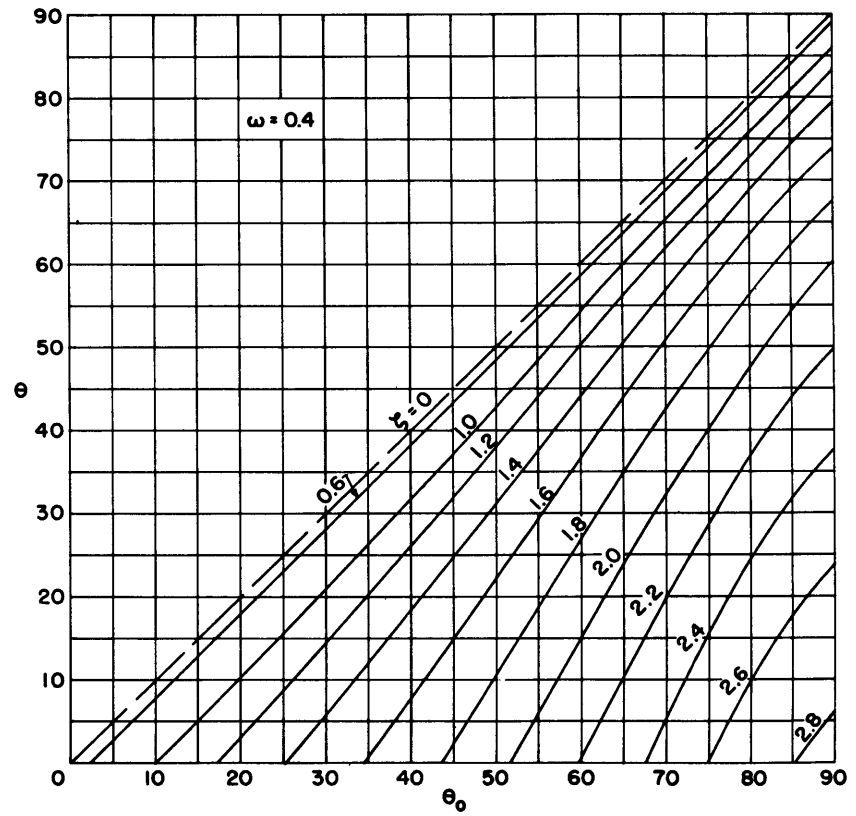


Figure 10 -  $\theta$  Versus  $\theta_0$  for  $\omega = 0.4$  (No End Loading)

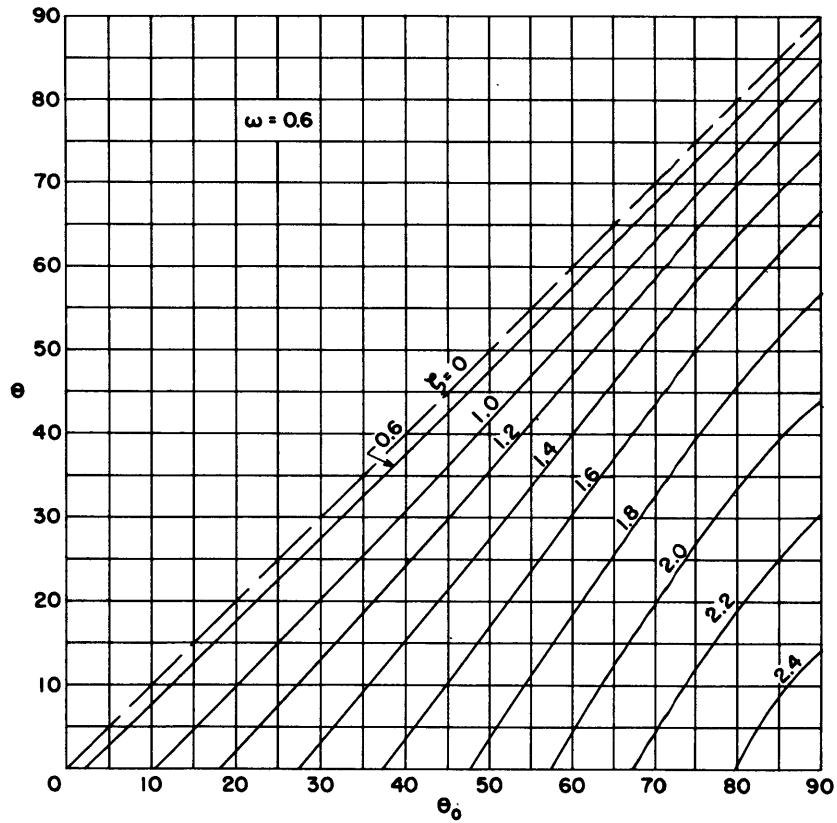


Figure 11 -  $\theta$  Versus  $\theta_0$  for  $\omega = 0.6$  (No End Loading)

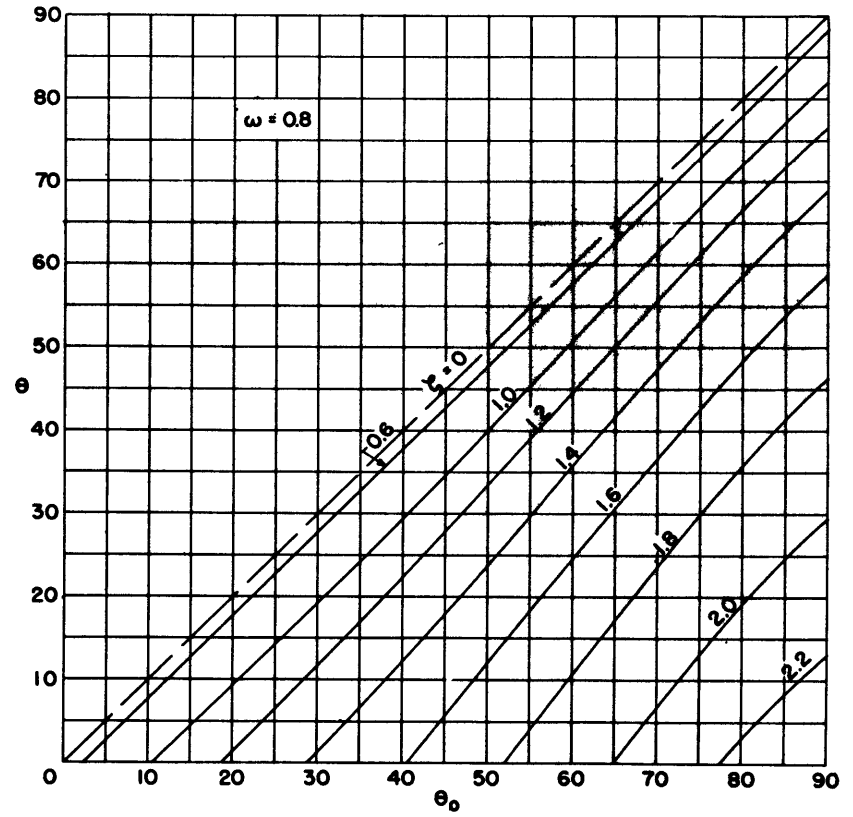


Figure 12 -  $\theta$  Versus  $\theta_0$  for  $\omega = 0.8$  (No End Loading)

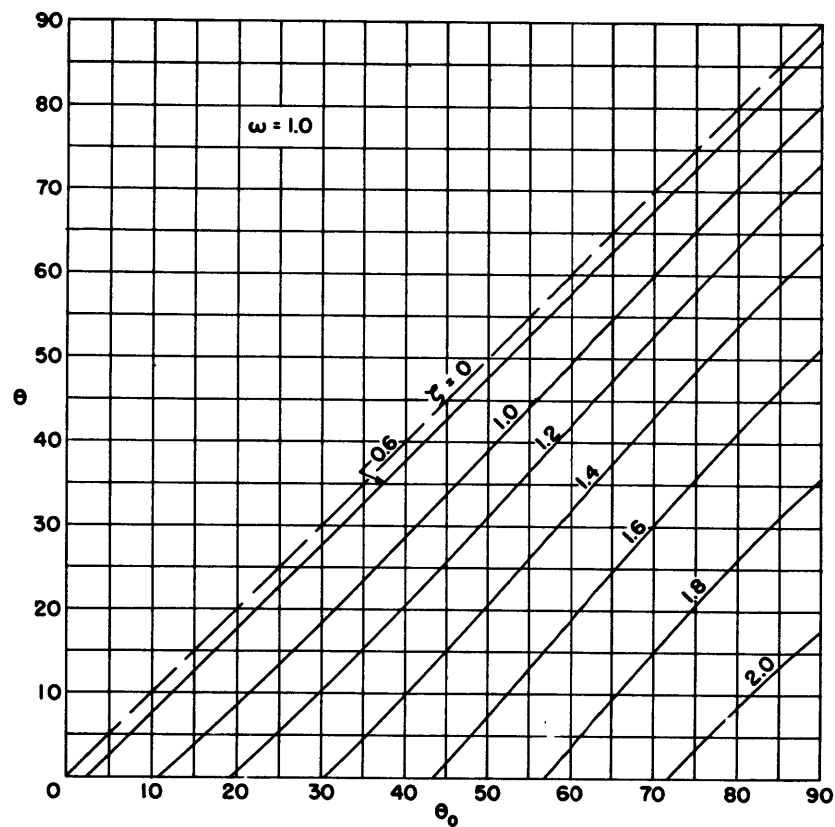


Figure 13 -  $\theta$  Versus  $\theta_0$  for  $\omega = 1.0$  (No End Loading)

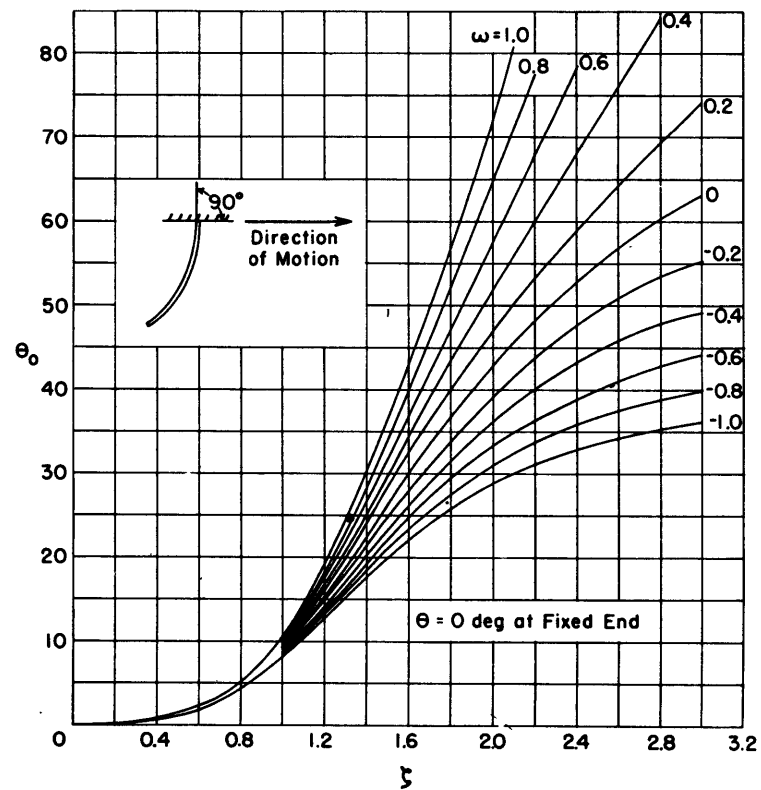


Figure 14 -  $\theta$  Versus  $\zeta$  with  $\omega$  as Parameter for Fixed End Normal to Direction of Motion (No End Loading)

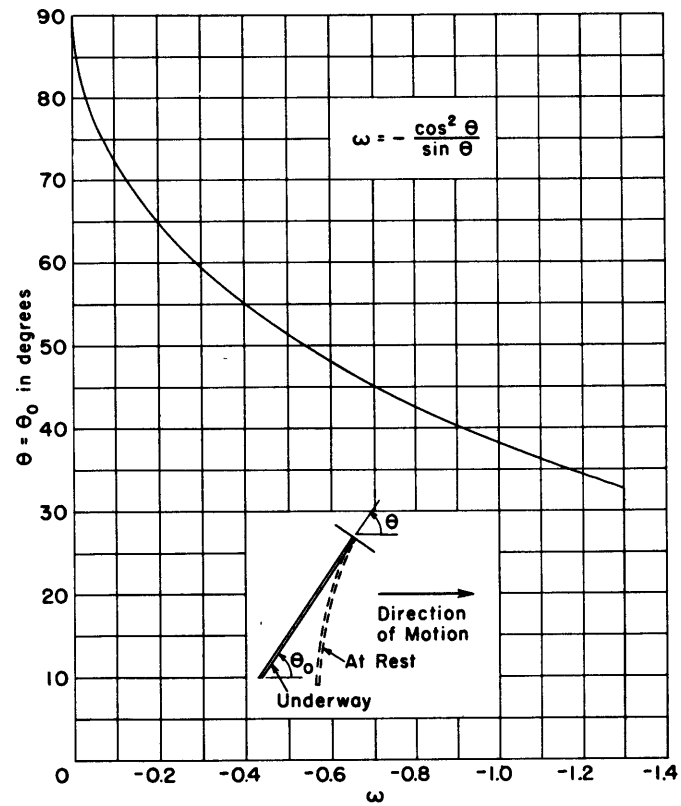


Figure 15. -  $\theta = \theta_0$  Versus  $\omega$  for Condition of No Bending Stress (No End Loading)

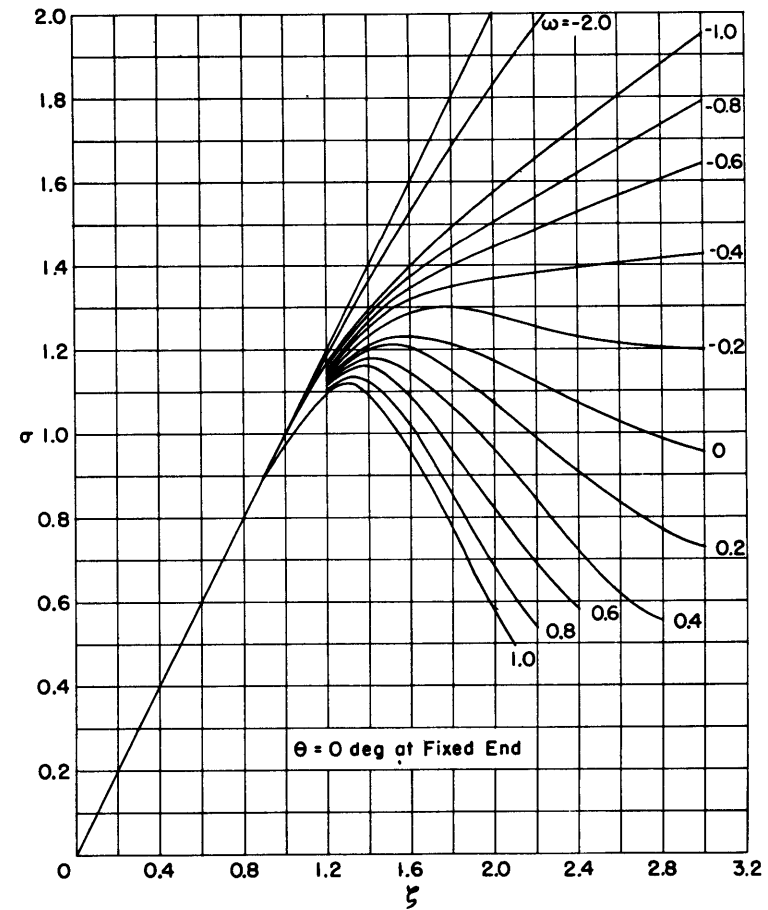


Figure 16 - Non-Dimensional Shear Force  $\sigma$  as a Function of  $\zeta$  for the Fixed End Normal to the Direction of Motion (No End Loading)

TABLE 2

Values of  $\sigma$  for Cantilevers with No End Loading

| $\omega \backslash \zeta$ | 1.0   | 0.8   | 0.6   | 0.4   | 0.2   | 0     | -0.2  | -0.4  | -0.6  | -0.8  | -1.0  |
|---------------------------|-------|-------|-------|-------|-------|-------|-------|-------|-------|-------|-------|
| 0                         | 0     | 0     | 0     | 0     | 0     | 0     | 0     | 0     | 0     | 0     | 0     |
| 0.2                       | 0.2   | 0.2   | 0.2   | 0.2   | 0.2   | 0.2   | 0.2   | 0.2   | 0.2   | 0.2   | 0.2   |
| 0.4                       | 0.4   | 0.4   | 0.4   | 0.4   | 0.4   | 0.4   | 0.4   | 0.4   | 0.4   | 0.4   | 0.4   |
| 0.6                       | 0.6   | 0.6   | 0.6   | 0.6   | 0.6   | 0.6   | 0.6   | 0.6   | 0.6   | 0.6   | 0.6   |
| 0.8                       | 0.8   | 0.8   | 0.8   | 0.8   | 0.8   | 0.8   | 0.8   | 0.8   | 0.8   | 0.8   | 0.8   |
| 1.0                       | 0.970 | 0.075 | 0.978 | 0.982 | 0.985 | 0.985 | 0.985 | 0.988 | 0.989 | 0.990 | 0.990 |
| 1.2                       | 1.10  | 1.105 | 1.11  | 1.12  | 1.129 | 1.132 | 1.14  | 1.15  | 1.16  | 1.163 | 1.17  |
| 1.4                       | 1.088 | 1.122 | 1.16  | 1.178 | 1.20  | 1.21  | 1.235 | 1.255 | 1.269 | 1.28  | 1.294 |
| 1.6                       | 0.955 | 1.021 | 1.09  | 1.144 | 1.202 | 1.23  | 1.288 | 1.32  | 1.348 | 1.373 | 1.40  |
| 1.8                       | 0.775 | 0.855 | 0.958 | 1.068 | 1.15  | 1.215 | 1.30  | 1.35  | 1.40  | 1.443 | 1.49  |
| 2.0                       | 0.575 | 0.675 | 0.825 | 0.96  | 1.073 | 1.172 | 1.28  | 1.37  | 1.445 | 1.50  | 1.575 |
| 2.2                       |       | 0.540 | 0.685 | 0.84  | 0.988 | 1.128 | 1.255 | 1.384 | 1.485 | 1.56  | 1.655 |
| 2.4                       |       |       | 0.580 | 0.72  | 0.906 | 1.072 | 1.230 | 1.395 | 1.53  | 1.62  | 1.73  |
| 2.6                       |       |       |       | 0.614 | 0.835 | 1.028 | 1.210 | 1.406 | 1.57  | 1.68  | 1.805 |
| 2.8                       |       |       |       | 0.553 | 0.770 | 0.985 | 1.205 | 1.418 | 1.61  | 1.735 | 1.878 |
| 3.0                       |       |       |       |       | 0.729 | 0.955 | 1.20  | 1.425 | 1.645 | 1.79  | 1.95  |

and the moments from\*

$$\mu = \frac{cM}{EI} = \int_0^{\zeta} \sin \theta_y \left[ \int_0^{\gamma} \cos^2 \theta(\mu) \sin \theta(\mu) d\mu + \omega \zeta \right] d\zeta \quad [13]$$

$$+ \int_0^{\zeta} \cos \theta_y \left[ \int_0^{\gamma} \cos^3 \theta(\mu) d\mu \right] d\zeta$$

Values of  $\sigma$  and  $\mu$  as functions of  $\zeta$  with  $\omega$  as parameter are given in Tables 2 and 3 and plotted in Figures 16 and 17 for the case of a cantilever with no loading at the free end. These values were obtained by numerical integration of Equations [12] and [13].

To the degree of approximation used herein, the bending stress, obtained from the bending moment formula and the usual linearizing assumptions, is given by

\*The shears and moments are represented in these integral forms since greater over-all accuracy will be obtained than by taking first and second derivatives of an approximating function with only a limited number of terms.

TABLE 3

Values of  $\mu$  for Cantilever with No End Loading

| $\zeta \backslash \omega$ | 1.0    | 0.8    | 0.6    | 0.4    | 0.2    | 0       | -0.2   | -0.4   | -0.6    | -0.8   | -1.0   |
|---------------------------|--------|--------|--------|--------|--------|---------|--------|--------|---------|--------|--------|
| 0                         | 0      | 0      | 0      | 0      | 0      | 0       | 0      | 0      | 0       | 0      | 0      |
| 0.2                       | 0.020  | 0.020  | 0.020  | 0.020  | 0.020  | 0.020   | 0.020  | 0.020  | 0.020   | 0.020  | 0.020  |
| 0.4                       | 0.080  | 0.080  | 0.080  | 0.080  | 0.080  | 0.080   | 0.080  | 0.080  | 0.080   | 0.080  | 0.080  |
| 0.6                       | 0.180  | 0.180  | 0.180  | 0.180  | 0.180  | 0.180   | 0.180  | 0.180  | 0.180   | 0.180  | 0.180  |
| 0.8                       | 0.320  | 0.320  | 0.320  | 0.320  | 0.320  | 0.320   | 0.320  | 0.320  | 0.320   | 0.320  | 0.320  |
| 1.0                       | 0.4954 | 0.4982 | 0.4988 | 0.4990 | 0.4992 | 0.4993  | 0.4994 |        |         |        |        |
| 1.2                       | 0.7048 | 0.7057 | 0.7062 | 0.7094 | 0.7100 | 0.7115  | 0.7120 | 0.7126 | 0.7130  | 0.7145 | 0.7179 |
| 1.4                       | 0.9272 | 0.9309 | 0.9380 | 0.9412 | 0.9432 | 0.9479  | 0.9520 | 0.9535 | 0.9575  | 0.9582 | 0.9625 |
| 1.6                       | 1.1256 | 1.1457 | 1.165  | 1.1722 | 1.1807 | 1.1936  | 1.2054 | 1.2125 | 1.2165  | 1.2243 | 1.2309 |
| 1.8                       | 1.2964 | 1.3312 | 1.3622 | 1.3911 | 1.4182 | 1.4393  | 1.4647 | 1.4797 | 1.4918  | 1.5041 | 1.5168 |
| 2.0                       | 1.432  | 1.4888 | 1.5400 | 1.5927 | 1.6424 | 1.67725 | 1.7215 | 1.7485 | 1.77605 | 1.7993 | 1.8249 |
| 2.2                       |        | 1.5836 | 1.6923 | 1.7726 | 1.8485 | 1.9037  | 1.9785 | 2.0225 | 2.0709  | 2.1053 | 2.1498 |
| 2.4                       |        |        | 1.8188 | 1.9308 | 2.0386 | 2.1261  | 2.225  | 2.3107 | 2.3688  | 2.4245 | 2.4884 |
| 2.6                       |        |        |        | 2.0627 | 2.2080 | 2.3317  | 2.4682 | 2.5794 | 2.6798  | 2.7523 | 2.8395 |
| 2.8                       |        |        |        | 2.1797 | 2.370  | 2.5342  | 2.7102 | 2.8602 | 2.9968  | 3.0945 | 3.2063 |
| 3.0                       |        |        |        |        | 2.5174 | 2.7268  | 2.9507 | 3.1437 | 3.3220  | 3.4463 | 3.5873 |

$$\psi = \frac{S_{bend}}{E} \times \frac{s}{h} = \frac{1}{2} \mu \zeta \quad [14]$$

where  $S_{bend}$  is the bending stress and  $h$  is the depth of the beam in the plane of bending. Values of  $\psi$  as a function of  $\zeta$  with  $\omega$  as parameter are given in Table 4 and plotted in Figure 18.

The tensile force may be obtained from Equations [1] and [2].

### COMPARISON WITH EXPERIMENTAL RESULTS

Experiments to check the accuracy of the results were conducted with rods of circular section and lengths of 5, 9, and 10 feet. Most data were obtained with the 10-foot rod. Circular rods were chosen primarily because of the availability of drag coefficients  $C_D$ . However, since drag coefficients are available only for non-vibrating cylinders, it was possible to utilize only data obtained with rods 1/8-inch and 1/4-inch in diameter. Larger rods were tested but the natural frequencies were in the range of vortex frequencies and large vibrations occurred so that these data could not be analyzed.

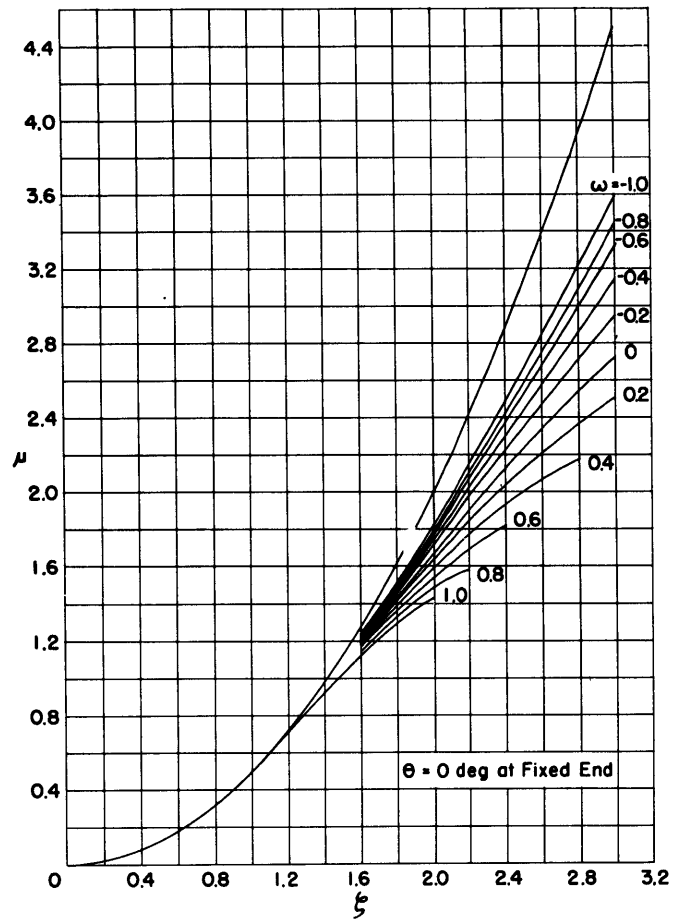


Figure 17 - Non-Dimensional Moment  $\mu$  as a Function of  $\zeta$  for Fixed End Normal to Direction of Motion (No End Loading)

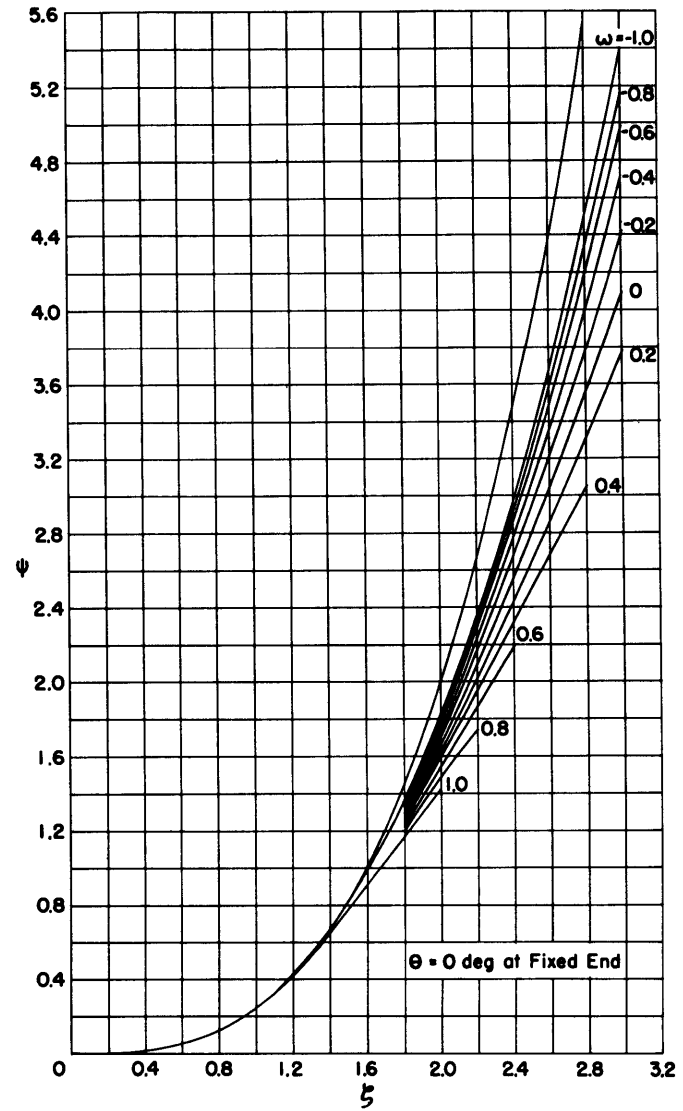


Figure 18 - Non-Dimensional Bending Stress  $\psi$  as a Function of  $\zeta$  for Fixed End Normal to Direction of Motion (No End Loading)

TABLE 4

Values of  $\psi$  for Cantilever with No End Loading

| $\xi$ | 1.0     | 0.8     | 0.6     | 0.4     | 0.2     | 0       | -0.2    | -0.4    | -0.6    | -0.8    | -1.0    |
|-------|---------|---------|---------|---------|---------|---------|---------|---------|---------|---------|---------|
| 0     | 0       | 0       | 0       | 0       | 0       | 0       | 0       | 0       | 0       | 0       | 0       |
| 0.2   | 0.002   | 0.002   | 0.002   | 0.002   | 0.002   | 0.002   | 0.002   | 0.002   | 0.002   | 0.002   | 0.002   |
| 0.4   | 0.016   | 0.016   | 0.016   | 0.016   | 0.016   | 0.016   | 0.016   | 0.016   | 0.016   | 0.016   | 0.016   |
| 0.6   | 0.054   | 0.054   | 0.054   | 0.054   | 0.054   | 0.054   | 0.054   | 0.054   | 0.054   | 0.054   | 0.054   |
| 0.8   | 0.128   | 0.128   | 0.128   | 0.128   | 0.128   | 0.128   | 0.128   | 0.128   | 0.128   | 0.128   | 0.128   |
| 1.0   | 0.2477  | 0.2491  | 0.2494  | 0.2495  | 0.2496  | 0.24965 | 0.2497  |         |         |         |         |
| 1.2   | 0.42288 | 0.42342 | 0.42372 | 0.42564 | 0.4260  | 0.4268  | 0.4272  | 0.42756 | 0.4278  | 0.4287  | 0.43074 |
| 1.4   | 0.64904 | 0.65163 | 0.6566  | 0.65884 | 0.66024 | 0.66353 | 0.6664  | 0.66745 | 0.67025 | 0.67074 | 0.67375 |
| 1.6   | 0.90048 | 0.91656 | 0.9320  | 0.93776 | 0.94456 | 0.95488 | 0.96432 | 0.9700  | 0.9732  | 0.97944 | 0.98472 |
| 1.8   | 1.16676 | 1.19808 | 1.22598 | 1.2520  | 1.27638 | 1.2954  | 1.3182  | 1.3317  | 1.3426  | 1.3567  | 1.3651  |
| 2.0   | 1.4226  | 1.4888  | 1.540   | 1.5927  | 1.6424  | 1.67725 | 1.7215  | 1.7485  | 1.77605 | 1.7993  | 1.8249  |
| 2.2   |         | 1.74196 | 1.8615  | 1.9499  | 2.0333  | 2.0941  | 2.17635 | 2.225   | 2.278   | 2.316   | 2.3648  |
| 2.4   |         |         | 2.1826  | 2.317   | 2.4463  | 2.5513  | 2.670   | 2.7728  | 2.8426  | 2.9094  | 2.9861  |
| 2.6   |         |         |         | 2.6815  | 2.8704  | 3.0312  | 3.2087  | 3.3532  | 3.4837  | 3.578   | 3.6913  |
| 2.8   |         |         |         | 3.0516  | 3.318   | 3.548   | 3.7943  | 4.0043  | 4.1955  | 4.3323  | 4.489   |
| 3.0   |         |         |         |         | 3.776   | 4.090   | 4.426   | 4.715   | 4.983   | 5.1694  | 5.381   |

The towing arrangement is shown schematically in Figure 19. The test specimen was fastened to the lower end of a strut of ogival section which in turn was bolted to the towing girder of the carriage over the deep-water basin of the David Taylor Model Basin. The drag force was measured by the scale arrangement indicated. The fine deviation from equilibrium was indicated on tape on the revolving drum. Speeds were obtained by a chronograph arrangement also recording on the drum. The resolution in speed is 0.01 knot and in drag is 0.005 pound. Because of the tare drag of the ogival strut, however, the accuracy at the low speeds was much less than these values. For the data presented, it is estimated that the error in drag of the test specimen may be as high as  $\pm 5$  percent.

Since all tests were made with the rods initially vertical, i.e.,  $\theta_f = 0$ , the measured drag was equal to the total shear. Thus, the total drag  $S$  is found from [12],

$$\sigma = \frac{S}{cR} = \int_0^{\xi} \cos^3 \theta d\xi \quad [15]$$

The experimental values were reduced using the following constants:  $E = 29 \times 10^6$  pounds per square inch (obtained from a tensile test of several specimens), and  $C_D = 1.2$ . The weight of the specimen is, of course, its weight in the liquid. Because of the manner in which the towing tests were conducted, the rods were towed through fluid having a fairly high degree



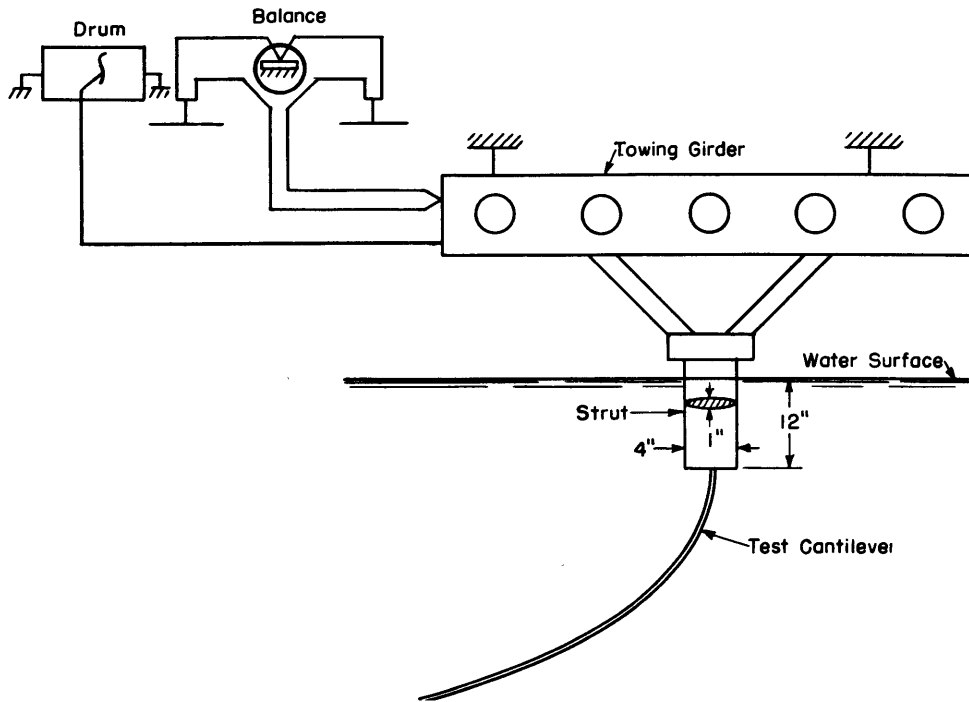


Figure 19 - Diagram of Experimental Arrangement

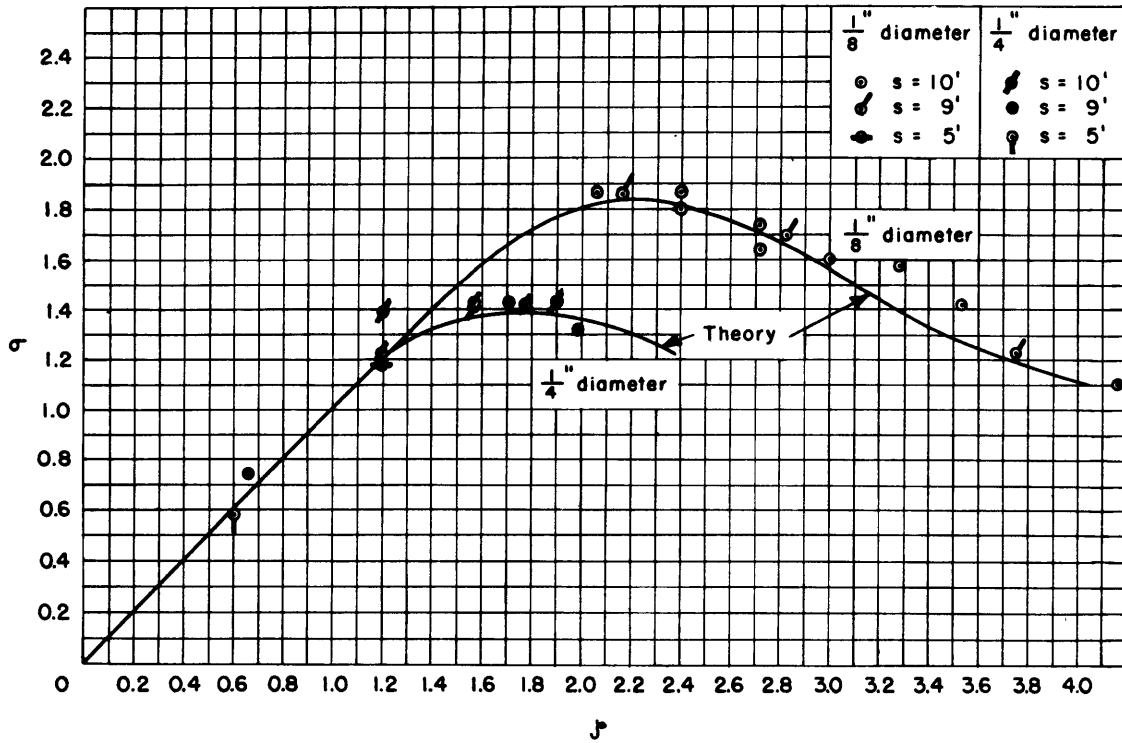


Figure 20 - Comparison of Theoretical and Experimental Results

of residual turbulence induced during the previous passage. Thus, over the entire range of test Reynolds numbers, a constant value of  $C_D = 1.2$  could be used.<sup>8</sup>

The reduced experimental results are compared with the theoretical predictions in Figure 20. Considering the errors inherent in the assumptions made and in the experiments, the agreement is quite satisfactory. The angle  $\theta_0$  corresponding to the highest value of  $\zeta$  was about 63 degrees.

### CONCLUDING REMARKS

Coarse observations during the experiments of the smallest radius of curvature of the bars just before failure (of the order of 50 rod diameters) indicate that the linearizing assumptions that were made were justified. Since the yield points of the specimens were about 70,000 pounds per square inch, it appears that the present results will be adequate within the elastic range of most engineering materials having an approximately linear stress-strain curve.

### ACKNOWLEDGMENTS

Tests to determine elastic moduli and yield points were carried out by Mr. Edward H. Boblits of the Structural Mechanics Laboratory.

### REFERENCES

1. Landweber, L. and Protter, M.H., "The Shape and Tension of a Light, Flexible Cable in a Uniform Current," TMB Report 533, October 1944.
2. Pode, Leonard, "Tables for Computing the Equilibrium Configuration of a Flexible Cable in a Uniform Stream," TMB Report 687, March 1951.
3. Glauert, H., "The Form of a Heavy Flexible Cable Used for Towing a Heavy Body Below an Airplane," ARC R & M Report 1592, February 1934.
4. Pode, Leonard, "An Experimental Investigation of the Hydrodynamic Forces on Stranded Cables," TMB Report 713, May 1950.
5. Bickley, W.F., "The Heavy Elastica," Phil. Mag. and Jour. of Sci., Vol. 17, 1934, pp. 603-614.
6. Seth, B.R., "Finite Strain in Elastic Problems," Phil. Trans. Roy. Soc. London, Ser. A, Vol. 234, 1934-35, pp. 231-264.
7. McLachlan, N.W., "Ordinary Non-Linear Differential Equations in Engineering and Physical Science," Oxford Univ. Press, 1950, pp. 174-178.
8. Schiller, L. and Linke, W., "Druck-und Reibungswiderstand des Zylinders bei Reynoldsen Zahlen 5000 bis 40,000," Zeit. Flugtechnik und Motorluftschiffahrt, Vol. 24, 193, 1933.

## APPENDIX

COEFFICIENTS OF EQUATION [8] FOR CANTILEVER WITH END LOADS  
 $T_0$  AND  $S_0$  AND MOMENT  $M_0$ 

$$\theta(0) = \theta_0$$

$$\theta'(0) = \mu_0$$

$$\theta''(0) = -\sigma_0$$

$$\theta'''(0) = \mu_0 \tau_0 - \cos^2 \theta_0 - \omega \sin \theta_0$$

$$\theta^{IV}(0) = \sigma_0 (\mu_0^2 - \tau_0) + 2\mu_0 \sin \theta_0 \cos \theta_0 - 2\omega \mu_0 \cos \theta_0$$

$$\begin{aligned} \theta^V(0) = & -\mu_0 (\tau_0^2 + 3\sigma_0^2) + \tau_0 \theta''' + \mu_0^2 (3 \cos^2 \theta_0 - 2 \sin^2 \theta_0) \\ & - 2\sigma_0 \sin \theta_0 \cos \theta_0 + 3\omega (\mu_0^2 \sin \theta_0 + \sigma_0 \cos \theta_0) \end{aligned}$$

$$\begin{aligned} \theta^{VI}(0) = & \sigma_0 (3\sigma_0^2 - \mu_0^4 + 6\tau_0 \mu_0^2) - \mu_0 \sigma_0 (11 \cos^2 \theta_0 - 6 \sin^2 \theta_0) \\ & - 10\mu_0^3 \sin \theta_0 \cos \theta_0 + \theta''' (4\mu_0 \sigma_0 + 2 \sin \theta_0 \cos \theta_0) \\ & + \omega (12\mu_0 \sigma_0 \sin \theta_0 + 4\mu_0^3 \cos \theta_0 - 4\theta''' \cos \theta_0) \end{aligned}$$

$$\begin{aligned} \theta^{VII}(0) = & \mu_0 (\tau_0 \mu_0^4 - 15\tau_0 \sigma_0^2 + 10\mu_0^2 \sigma_0^2) + \sigma_0^2 (14 \cos^2 \theta_0 - 6 \sin^2 \theta_0 + 64\mu_0^2 \sigma_0 \sin \theta_0 \cos \theta_0) \\ & + \mu_0^4 (10 \sin^2 \theta_0 - 11 \cos^2 \theta_0) + \theta''' (-10\tau_0 \mu_0^2 - 10\sigma_0^2 + 17\mu_0 \cos^2 \theta_0 - 8\mu_0 \sin^2 \theta_0) \\ & + \theta^{IV} (5\mu_0 \sigma_0 + 2 \sin \theta_0) + \tau_0 \theta^V + \omega (20\mu_0 \theta''' \sin \theta_0 - 5\theta^{IV} \cos \theta_0 \\ & + 15\sigma_0 \sin \theta_0 - 30\mu_0^2 \sigma_0 \cos \theta_0 - 5\mu_0^4 \sin \theta_0) \end{aligned}$$

$$\begin{aligned}
\theta^{V'''}(0) = & \sigma_0 (15 \tau_0 \sigma_0^2 - 15 \tau_0 \mu_0^4 + \mu_0^6 - 45 \mu_0^2 \sigma_0^2) - \mu_0^3 \sigma_0 (104 \sin^2 \theta_0 - 118 \cos^2 \theta_0) \\
& + \mu_0 (42 \mu_0^4 \sin \theta_0 \cos \theta_0 - 168 \sigma_0^2 \sin \theta_0 \cos \theta_0) - 114 \mu_0^2 \theta''' \sin \theta_0 \cos \theta_0 \\
& + \sigma_0 \theta''' (60 \tau_0 \mu_0 - 20 \mu_0^3 + 10 \theta''' + 20 \sin^2 \theta_0 - 55 \cos^2 \theta_0) \\
& + \theta^{IV} (-15 \tau_0 \mu_0^2 - 15 \sigma_0^2 + 24 \mu_0 \cos^2 \theta_0 - 10 \mu_0 \sin^2 \theta_0) \\
& + \theta^V (6 \mu_0 \sigma_0 + 2 \sin \theta_0 \cos \theta_0) + \tau_0 \theta^{V'} + \omega \theta''' (60 \mu_0^2 \cos \theta_0 - 60 \sigma_0 \sin \theta_0) \\
& + \omega (30 \mu_0 \theta^{IV} \sin \theta_0 - 6 \theta^V \cos \theta_0 - 6 \mu_0^5 \cos \theta_0 + 90 \mu_0 \sigma_0^2 \cos \theta_0) \\
& + 60 \mu_0^3 \sigma_0 \sin \theta_0
\end{aligned}$$

$$\begin{aligned}
\theta^{IX}(0) = & \sigma_0 (105 \mu_0^3 \sigma_0 \tau_0 - 21 \mu_0^5 \sigma_0 + 105 \sigma_0^3 \mu_0 + 168 \sigma_0^2 \sin \theta_0 \cos \theta_0 \\
& - 654 \mu_0 \cos \theta_0 \sin \theta_0) + \mu_0 \sigma_0^2 (480 \sin^2 \theta_0 - 567 \cos^2 \theta_0) \\
& - \mu_0^6 (43 \cos^2 \theta_0 - 42 \sin^2 \theta_0) + \theta''' (35 \tau_0 \mu_0^4 + 210 \sigma_0^2 \mu_0^2 - 105 \tau_0 \sigma_0^2) \\
& + 714 \mu_0 \sigma_0 \sin \theta_0 \cos \theta_0 + 228 \mu_0^3 \sin^2 \theta_0 - 252 \mu_0^3 \cos \theta_0 \\
& + (\theta''')^2 (-70 \tau_0 \mu_0 + 65 \cos^2 \theta_0 - 20 \sin^2 \theta_0) + 35 \sigma_0 \theta''' \theta^{IV} \\
& + \theta^{IV} (105 \tau_0 \mu_0 \sigma_0 - 35 \sigma_0 \mu_0^3 + 30 \sigma_0 \sin^2 \theta_0 - 94 \sigma_0 \cos^2 \theta_0 - 182 \sigma_0^2 \sin \theta_0 \cos \theta_0) \\
& + \theta^V (-21 \tau_0 \mu_0^2 - 21 \sigma_0^2 + 32 \mu_0 \cos^2 \theta_0 - 12 \mu_0 \sin^2 \theta_0) + \theta^{V''} \tau_0 \\
& + \theta^{V'} (7 \sigma_0 \mu_0 + 2 \sin \theta_0 \cos \theta_0) + \omega \theta^{IV} (105 \mu_0^2 \cos \theta_0 - 105 \sigma_0 \sin \theta_0) \\
& + \omega (42 \mu_0 \theta^V \sin \theta_0 - 70 \theta^{V'} \cos \theta_0 - 105 \sigma_0^3 \cos \theta_0 - 315 \mu_0^2 \sigma_0^2 \sin \theta_0) \\
& + 105 \mu_0^4 \sigma_0 \cos \theta_0 + 7 \mu_0^6 \sin \theta_0
\end{aligned}$$

## INITIAL DISTRIBUTION

### Copies

- 22 Chief, Bureau of Ships, Technical Library (Code 327), for distribution:
- 10 Technical Library
  - 2 Research (Code 300)
  - 2 Applied Science (Code 370)
  - 2 Preliminary Design (Code 420)
  - 2 Countermeasures (Code 520)
  - 1 Propeller and Shafting (Code 554)
  - 2 Antenna Systems (Code 838)
  - 1 Sonar Systems (Code 845)
- 2 Chief, Bureau of Ordnance, Underwater Ordnance (Re6a), Attn: Dr. F.A. Maxfield
- 2 Chief, Bureau of Ordnance, Code Re3, Attn: Dr. A. Miller
- 3 Chief of Naval Research
- 2 Fluid Mechanics (N426)
  - 1 Undersea Warfare (466)
- 2 Commander, U.S. Naval Ordnance Laboratory, White Oak, Silver Spring 19, Md.
- 2 Commander, U.S. Naval Ordnance Test Station, Hydrodynamics Office, Pasadena, Calif.
- 4 Commanding Officer and Director, U.S. Navy Underwater Sound Laboratory, New London, Conn.
- 2 Commanding Officer and Director, U.S. Navy Electronics Laboratory, San Diego 52, Calif.
- 1 Chief, Bureau of Aeronautics, Aero and Hydrodynamics (DE-3)
- 2 Director, National Advisory Committee for Aeronautics, 1724 F St., N.W., Washington, D.C.
- 2 Director, Iowa Institute of Hydraulic Research, State University of Iowa, Iowa City, Iowa
- 2 Director, Hydrodynamics Laboratory, California Institute of Technology, Pasadena 4, Calif.
- 2 Dr. J.M. Robertson, Ordnance Research Laboratory, Pennsylvania State College, State College, Pa.
- 1 Captain R. Brard, Directeur, Bassin d'Essais des Carenes, 6 Boulevard Victor, Paris (15e), France
- 1 Dr. L. Malavard, Office National d'Etudes et de Recherches Aéronautiques, 25 Avenue de la Division - Le Clerc, Chatillon, Paris, France
- 1 Gen.Ing. U. Pugliese, Presidente, Istituto Nazionale per Studi ed Esperienze di Architettura Navale, via della Vasca Navale 89, Rome, Italy

## Copies

- 1 Sr. M. Acevedo y Campoamor, Director, Canal de Experiencias Hidrodinámicas, El Pardo, Madrid, Spain
- 1 Dr. J. Dieudonné, Directeur, Institut de Recherches de la Construction Navale, 1 Boulevard Haussmann, Paris (9e), France
- 1 Prof. L. Troost, Superintendent, Nederlandsh Scheepsbouwkundig Proefstation, Haagsteeg 2, Wageningen, The Netherlands
- 1 Prof. J.K. Lunde, Skipsmodelltanken, Tyholt Trondheim, Norway
- 1 Prof. H. Nordstrom, Director, Statens Skeppsprovvningsanstalt, Göteborg 24, Sweden
- 1 Dr. S.L. Smith, Director, British Shipbuilding Research Association, 5 Chesterfield Gardens, Curzon Street, London, W.1, England
- 1 Dr. J.F. Allan, Superintendent, Ship Division, National Physical Laboratory, Teddington, Middlesex, England
- 9 British Joint Services Mission (Navy Staff), P.O. Box 165, Benjamin Franklin Station, Washington, D.C.
- 1 Dr. G.P. Weinblum, Edmund Siemens Allee 1, Universitaet, Hamburg, Germany

MIT LIBRARIES

DUPL



3 9080 02754 1538

INSPECTOR OF NAVAL MATERIAL  
RECEIVED  
MAR 25 1953  
BOSTON, MASS.  
5074

I. N. M.  
RECEIVED  
APR 1 1953  
927867  
Development Control Officer  
M. I.